Reversible Catalytic Reactions and the Stability of Ti Surface Defects in $NaAlH_4$

Kewu Bai, Pei Shan Emmeline Yeo, and Ping Wu*

Institute of High Performance Computing, 1 Fusionopolis Way, #16-16 Connexis, Singapore 138632

Received June 13, 2008. Revised Manuscript Received October 23, 2008

Despite many experimental and theoretical studies, the origin of the catalytic role of the Ti catalyst in the reversible dehydrogenation of $NaAlH_4$ has been a controversial topic for many years. In this paper, density functional theory and phase equilibrium calculations are used to study the surface defect stabilities of $NaAlH_4$ during dehydrogenation and rehydrogenation cycles. A Ti−H−Al cluster resulting from the Ti substitution of Al at the (001) subsurface layer of $NaAlH_4$ is identified as the most stable surface defect. An interstitial H in this cluster enhances the Ti−Al bonds and weakens the Al−H bonds simultaneously. The large difference in the formation enthalpy of this cluster under hydrogen-poor and hydrogen-rich conditions indicates that the concentration of these Ti−H−Al clusters on the $NaAlH_4$ (001) surface can be mediated by the hydrogenation and dehydrogenation cycles, which is responsible for the reversible catalytic behavior of the Ti catalyst.

Introduction

The design of new catalysts to improve the reversible dehydrogenation of hydrogen storage materials is viewed a challenge for the hydrogen storage industry, and this relies heavily on the understanding of the dehydrogenation mechanism of current transition-metal-catalyzed hydrogen storage materials.[1] Hence, the findings of Bogdanovic and Schwickardi, [2] that Ti-doped sodium alanates ($NaAlH_4$) could reversibly release and absorb hydrogen, spurred much research work on the mechanism of hydrogen release and uptake in transition-metal-doped $NaAlH_4$. Many experimental studies, mainly by means of X-ray synchrotron radiation, have been performed on Ti-doped $NaAlH_4$. [3−7] The consensus on the catalytically active Ti species is that the Ti-dopant is in a very slightly oxidized or zerovalent state and exhibits a nonordered and highly dispersed nature in $NaAlH_4$. This nature remains invariant during the dehydrogenation and hydrogenation cycles of $NaAlH_4$. [8] However, the exact location of the Ti species and the mechanism of its reversible catalytic behavior in $NaAlH_4$ are not well understood and has been in debate for years, even after different Ti-precursors such as Ti, [9] $TiAl_3$, [10] and TiH_2[11] instead of the commonly used $TiCl_3$[12] were used to probe the dehydrogenation/hydrogenation characteristics of $NaAlH_4$.

The debates surrounding the dehydrogenation mechanism of Ti in $NaAlH_4$ have presented a number of conflicting hypotheses. One such hypothesis proposes that Ti−Al clusters located on the $NaAlH_4$ surface lower the potential energy barrier to the formation of mobile AlH_3. [13] This hypothesis was partially supported by the observation of H_2 evolution during the doping process and X-ray absorption and electron microscopy studies of the Ti-doped $NaAlH_4$. [4,8,14] On the other hand, some studies conclude that Ti is not associated with the $NaAlH_4$ lattice at all. Rather, Ti concentrated on the surface of Al crystallites may serve as the most active site for the absorption of hydrogen, if one assumes that not all the Al atoms in the hydrogen-depleted material reacts to reform $NaAlH_4$. For example, theoretical and experimental results of Chaudhuri et al. [15] showed that Ti located on the Al(001) surface and subsurface layers could catalyze the dissociation of H_2 molecules and also aid in the diffusion of AlH_3 molecules, which helps in the reformation of $NaAlH_4$ after dehydrogenation. Similarly, X-ray diffraction

* Corresponding author. E-mail: wuping@ihpc.a-star.edu.sg.

(1) Schlapbach, L.; Züttel, A. *Nature* **2001**, *414*, 353–358.
(2) Bogdanovi, B.; Schwickardi, M. *J. Alloys Compd.* **1997**, *253−254*, 1–9.
(3) Bellosta von Colbe, J. M.; Bogdanovic, B.; Felderhoff, M.; Pommerin, A.; Schüth, F. *J. Alloys Compd.* **2004**, *370*, 104–109.
(4) Graetz, J.; Reilly, J. J.; Johnson, J.; Ignatov, A. Y.; Tyson, T. A. *Appl. Phys. Lett.* **2004**, *85*, 500–502.
(5) Leon, A.; Rothe, J.; Fichtner, M. *J. Phys. Chem. C* **2007**, *111*, 16664–16669.
(6) Léon, A.; Schild, D.; Fichtner, M. *J. Alloys Compd.* **2005**, *404−406*, 766–770.
(7) Weidenthaler, C.; Pommerin, A.; Felderhoff, M.; Bogdanović, B.; Schüth, F. *Phys. Chem. Chem. Phys.* **2003**, *5*, 5149–5153.
(8) Leon, A.; Kircher, O.; Fichtner, M.; Rothe, J.; Schild, D. *J. Phys. Chem. B* **2006**, *110*, 1192–1200.
(9) Wang, P.; Jensen, C. M. *J. Alloys Compd.* **2004**, *379*, 99–102.
(10) Kang, X. D.; Wang, P.; Song, X. P.; Yao, X. D.; Lu, G. Q.; Cheng, H. M. *J. Alloys Compd.* **2006**, *424*, 365–369.
(11) Kang, X. D.; Wang, P.; Cheng, H. M. *J. Phys. Chem. C* **2007**, *111*, 4879–4884.
(12) Bogdanovic, B.; Felderhoff, M.; Germann, M.; Hartel, M.; Pommerin, A.; Schuth, F.; Weidenthaler, C.; Zibrowius, B. *J. Alloys Compd.* **2003**, *350*, 246–255.
(13) Graetz, J.; Ignatov, A. Y.; Tyson, T. A.; Reilly, J. J.; Johnson, J. Characterization of the Local Titanium Environment in Doped Sodium Aluminum Hydride Using X-ray Absorption Spectroscopy. In *Materials for Hydrogen Storage*; Vogt, T., Stumpf, R., Heben, M., Robertson, I., Eds.; Materials Research Society: Warrendale, PA, 2005; Vol. 837, p 25.
(14) Canton, P.; Fichtner, M.; Frommen, C.; Leon, A. *J. Phys. Chem. B* **2006**, *110*, 3051–3054.
(15) Chaudhuri, S.; Graetz, J.; Ignatov, A.; Reilly, J. J.; Muckerman, J. T. *J. Am. Chem. Soc.* **2006**, *128*, 11404–11415.

10.1021/cm8016038 CCC: $40.75
Published on Web 11/24/2008

studies by Haiduc[16] concluded that the Ti formed a solid solution with elemental Al. However, electron microscopy studies by Léon et al. [17] on Ti-doped $NaAlH_4$ showed that Ti is not exclusively associated with Al, despite the presence of Al crystallites that are about 280 nm wide. Baldé et al. [18] merged the two above ideas, proposing that 30% of Ti are incorporated on the surface of Al crystallites and 70% of Ti occupied subsurface interstitials in the $NaAlH_4$ lattice. This, they argued, was a way in which the calculated Ti−Al coordination numbers could satisfy the values observed in their extended X-ray adsorption fine structure spectroscopy experiments. By using a two-step ball-milling method, Kang et al. [11] ruled out the possibility of a Ti−Al phase. Their hypothesis is that a localized metastable Al−H−Ti acts as an active site for the dissociation and recombination of H_2 molecules. This cluster, however, may fall below the detection limit of traditional analytical techniques.

It is this difficulty in identifying the catalytically active Ti species by experimental analytical techniques that has prompted the use of computational science to resolve the issue. In the earlier density functional theory (DFT) calculations, most of the studies had concentrated on the energetics of Ti atom substitution of Na and Al in the bulk lattice of $NaAlH_4$,[19−21] while the more recent DFT studies have focused on possible Ti locations in the $NaAlH_4$ surface. Using a slab model, Liu et al. [22] proposed that Ti atoms located in the interstitial sites of (001) and (100) $NaAlH_4$ surfaces are energetically favorable, while Vegge[23] suggested that Ti substituted Na on the (001) $NaAlH_4$ surface. In contrast, Marashdeh et al. [24] proposed that the Ti atoms may adsorb above Na sites on the surface, with the Na atoms displaced toward the subsurface region. The Ti atom then "unzips" the $NaAlH_4$ like a slider. Gunaydin et al. [25] recently analyzed the atomic processes occurring in $NaAlH_4$ and the changes to the chemical bond of hydrogen at dehydrogenation temperatures. They suggest that the bulk diffusion of Al species via AlH_3 is the rate-limiting step.

It can be seen that several important issues related to the reversible catalytic behavior of Ti in $NaAlH_4$ have not been confirmed or addressed yet. The first issue is regarding the exact location of Ti on the surface of $NaAlH_4$ and how it is involved in the phase transformation of $NaAlH_4$ to Na_3AlH_6. (It is reported that the first decomposition reaction of $NaAlH_4$ is $NaAlH_4 \leftrightarrow (1/3)Na_3AlH_6 + (2/3)Al + H_2$.)[26] The second issue is regarding the elucidation of the reversible dehydrogenation/hydrogenation mechanism of Ti-doped $NaAlH_4$.

To address the above issues, we extend our previous DFT calculation work[27] on Ti-doped $NaAlH_4$ to the surface defect calculations of (001) $NaAlH_4$. Our strategy is as follows: (i) first, we calculate the chemical potential limits of Na, Al, and H when assuming $NaAlH_4$ is in metastable phase equilibrium with Na_3AlH_6. This allows the calculated surface defect stability to be directly related to the dehydrogenation reaction of $NaAlH_4$ (See Methodology section for more details). [2] (ii) Second, we explore the stabilities of different Ti configurations on the $NaAlH_4$ (001) surface, where the Ti-defect formation enthalpy is described by density functional theory (DFT) calculations for the doped and undoped $NaAlH_4$ (001) surface slab and the calculated chemical potentials of the different species in step (i). Specifically, we correlate the formation enthalpy of the most stable Ti-defect to changes in the chemical potential of H during dehydrogenation and hydrogenation, which will give us insight into what happens to the Ti-defect in $NaAlH_4$ during those processes. Our calculations differ from the previous theoretical work [21,28,29] in that the chemical potentials, rather than total energies of the pure constituents of Ti-doped $NaAlH_4$ system, are used for the defect formation enthalpy calculations. These potentials are limited by the chemical environments of the Ti-doped $NaAlH_4$ dehydrogenation/hydrogenation processes. (iii) Having established the most stable Ti-defect, we then proceed to probe the bond changes in the surface slab with and without Ti-doping by electronic structure calculations. (iv) The most probable hypothesis of the reversible catalytic behavior of Ti is presented at the end.

Computational Methodology

The spin-polarized DFT calculations are performed using the Vienna ab initio simulation program (VASP) code[30] with the projector augmented wave (PAW) method.[31] The Perdew−Wang 91 (PW91) generalized gradient approximation (GGA)[32] is used for the exchange correlation functional. The Na $2s^2\ 2p^6\ 3s^1$ electrons, the Al $3s^2\ 3p^1$ electrons, the H $1s^1$ electron,and the Ti $3s^2\ 3p^6\ 3d^2\ 4s^2$ electrons are treated as valence electrons. As a first step, we calculate the bulk lattice property of $NaAlH_4$ using an energy cutoff of 700 eV for the plane waves and a $5 \times 5 \times 2$ gamma K-mesh. The optimized lattice parameters of $NaAlH_4$ are $a = 4.9695$ Å and $c = 11.1268$ Å. The internal atomic coordinates of H are $x = 0.2379$, $y = 0.3901$, and $z = 0.5441$. The calculated lattice parameters and hydrogen position coordinates of $NaAlH_4$ with PW91 agree with experimental data[33] and other theoretical studies.[34,35] They are also slightly closer to the

(16) Haiduc, A. G.; Stil, H. A.; Schwarz, M. A.; Paulus, P.; Geerlings, J. J. C. *J. Alloys Compd.* **2005**, *393*, 252–263.
(17) Léon, A.; Kircher, O.; Rösner, H.; Décamps, B.; Leroy, E.; Fichtner, M.; Percheron-Guégan, A. *J. Alloys Compd.* **2006**, *414*, 190–203.
(18) Baldé, C. P.; Stil, H. A.; van der Eerden, A. M. J.; Jong, K. P. d.; Bitter, J. H. *J. Phys. Chem. Chem. Phys.* **2007**, *111*, 2797–2802.
(19) Araujo, C. M.; Li, S.; Ahuja, R.; Jena, P. *Phys. Rev. B* **2005**, *72*, 165101–6.
(20) Íñiguez, J.; Yildirim, T.; Udovic, T. J.; Sulic, M.; Jensen, C. M. *Phys. Rev. B* **2004**, *70*, 060101.
(21) Lovvik, O. M.; Opalka, S. M. *Phys. Rev. B* **2005**, *71*, 054103–10.
(22) Liu, J.; Ge, Q. *J. Phys. Chem. B* **2006**, *110*, 25863–25868.
(23) Vegge, T. *Phys. Chem. Chem. Phys.* **2006**, *8*, 4853–4861.
(24) Marashdeh, A.; Olsen, R. A.; Lovvik, O. M.; Kroes, G. J. *J. Phys. Chem. C* **2007**, *111*, 8206–8213.
(25) Gunaydin, H.; Houk, K. N.; Ozolins, V. *Proc. Natl. Acad. Sci. U.S.A.* **2008**, *105*, 3673–3677.
(26) Gross, K. J.; Guthrie, S.; Takara, S.; Thomas, G. *J. Alloys Compd.* **2000**, *297*, 270–281.
(27) Bai, K.; Wu, P. *Appl. Phys. Lett.* **2006**, *89*, 201904–3.
(28) Araújo, C. M.; Ahuja, R.; Guillén, J. M. O.; Jena, P. *Appl. Phys. Lett.* **2005**, *86*, 251913.
(29) Iñiguez, J.; Yildirim, T. *Appl. Phys. Lett.* **2005**, *86*, 103109.
(30) Kresse, G. F., J. *Phys. Rev. B* **1996**, *54*, 11169–11186.
(31) Kresse, G.; Joubert, D. *Phys. Rev. B* **1999**, *59*, 1758.
(32) Perdew, J. P.; Wang, Y. *Phys. Rev. B* **1992**, *45*, 13244–13249.
(33) Hauback, B. C.; Brinks, H. W.; Jensen, C. M.; Murphy, K.; Maeland, A. J. *J. Alloys Compd.* **2003**, *358*, 142–145.

experimental results than those calculated using the Perdew, Burke, and Ernzerhof (PBE) functional.[36]

The optimized lattice parameters are used as a basis for construction of surface slabs of $NaAlH_4$ with and without the Ti-dopant. Among all the low index surfaces, the (001) surface of the conventional-cell $NaAlH_4$ is chosen to study the stability of the surface defect stability of T-doped $NaAlH_4$ because it has the lowest surface energy (see eq 1 below). [23,34] To avoid interactions between the defects and their periodic image, a four-layer, $3 \times 3 \times 1$ supercell slab of $NaAlH_4$ consisting of 216 atoms (36 formula units) is constructed. Convergence tests show that a vacuum layer thickness of 10 Å is sufficient. The positions of the ions in the two bottom layers of the surface slab are fixed to simulate the bulk layers of the surface, while the ionic coordinates of atoms at the two top layers are relaxed until the total residual force components acting on the ions are less than 0.03 eV/Å. Only the gamma *k*-point is used in the slab calculations, which is justified by the large size of the slab. The surface energy γ of the pure $NaAlH_4$ (001) surface is calculated by the equation formulated by Bottger[37] which ensures that the calculated surface energy converges with increasing layers for the slab:[23,34]

$$\gamma = (E^N_{\mathrm{Slab}} - N\Delta E_N)/A \qquad (1)$$

where E^N_{Slab} is the energy for a slab of N "layers", A is the area of the slab surface per slab unit cell (including both surfaces), and ΔE_N is the energy difference for a single layer between two slabs with different numbers of layers (i.e., $\Delta E_N = E^N_{\mathrm{Slab}} - E^{N-1}_{\mathrm{Slab}}$). The calculated surface energy for our $3 \times 3 \times 1$ $NaAlH_4$ surface slab is 0.159 J/m^2, which is comparable to the 0.153 J/m^2 calculated by Frankcombe and Løvvik[34] using VASP on a $2 \times 2 \times 1$ slab.

Next, we calculated the defect formation enthalpy of the surface defects involving different Ti configurations to determine the most stable one. Besides those reported in the literature, additional Ti configurations are taken into account for an extensive study of Ti surface defects in Ti-doped $NaAlH_4$ (001) surface. They are (a) models in which Ti atom substitutes Al in the surface or subsurface layer, denoted by $Ti^{\mathrm{surf}}_{\mathrm{Al}}$ and $Ti^{\mathrm{sub}}_{\mathrm{Al}}$,respectively; (b) models in which Ti atom substitutes Na in the surface or subsurface layer, denoted by $Ti^{\mathrm{surf}}_{\mathrm{Na}}$ and $Ti^{\mathrm{sub}}_{\mathrm{Na}}$, respectively; (c) models in which the Ti atoms are located at interstitial sites of the surface. The exact locations of these interstitial Ti atoms on the (001) $NaAlH_4$ slab are shown in Figure 1, where Ti atoms 1 ($Ti^{\mathrm{surf1}}_{i2\mathrm{AlH_4}}$) and 2 ($Ti^{\mathrm{surf2}}_{i2\mathrm{AlH_4}}$) refer to Ti atoms located at two different surface interstitial sites between two AlH_4^- units, Ti atoms 3 ($Ti^{\mathrm{surf}}_{i\mathrm{Na}}$) and 4 ($Ti^{\mathrm{surf}}_{i\mathrm{Al}}$) refer to Ti atoms located on top of Na or Al atoms on the surface, respectively, and Ti atoms 5 (Ti_i^{sub1}) and 6 (Ti_i^{sub2}) are located at two different subsurface interstitial sites; and (d) models in which Ti substitutes Al or Na in the subsurface layer with an interstitial H atom in the vicinity of the Ti atom, which are denoted by $Ti^{\mathrm{sub}}_{\mathrm{Al}} + H_i$ and $Ti^{\mathrm{sub}}_{\mathrm{Na}} + H_i$, respectively.

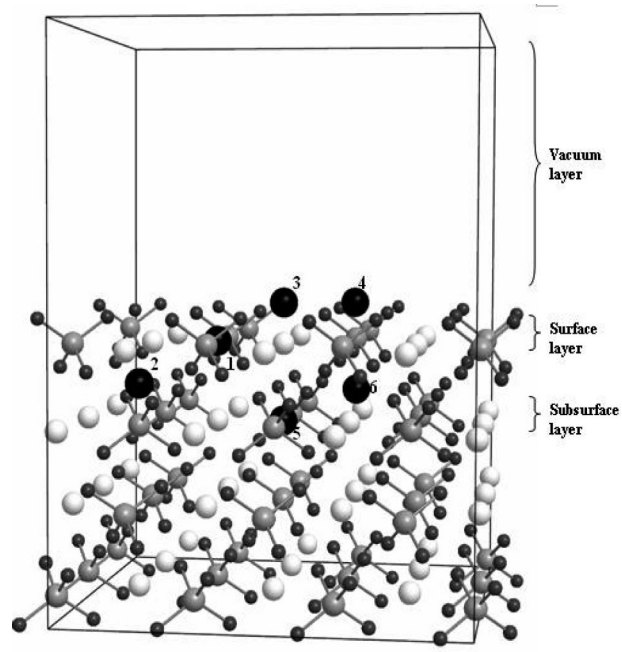

Figure 1. Surface slab of $NaAlH_4$ with Ti at different interstitial doping sites. The Ti atoms 1 ($Ti^{\mathrm{surf1}}_{i2\mathrm{AlH_4}}$) and 2 ($Ti^{\mathrm{surf2}}_{i2\mathrm{AlH_4}}$) are at surface interstitial sites between $2AlH_4^-$ units. The Ti atoms 3 ($Ti^{\mathrm{surf}}_{i\mathrm{Na}}$) and 4 ($Ti^{\mathrm{surf}}_{i\mathrm{Al}}$) are respectively located on top of Na and Al atoms on the surface. Ti atoms 5 (Ti_i^{sub1}) and 6 (Ti_i^{sub2}) are at the interstitial sites of the subsurface layer. Here, the small black balls, big black balls, gray balls, and white balls denote H, Ti, Al, and Na atoms, respectively.

The formation enthalpy of these defects was calculated by[38]

$$\Delta H_{\mathrm{f}}^{\mathrm{defect}} = E^{\mathrm{defect}}_{\mathrm{Slab}} - E_{\mathrm{Slab}} + \sum_{\alpha} n_\alpha \mu_\alpha + \Delta\mathrm{ZPE} \qquad (2)$$

where $E^{\mathrm{defect}}_{\mathrm{Slab}}$ and E_{Slab} are the total energies of the slabs with and without defect α, μ_α is the absolute value of the atomic chemical potential of α, and n_α is the number of the defect atoms; $n_\alpha = 1$ when an atom removed, and $n_\alpha = -1$ when an atom is added. ΔZPE is the zero point energy (ZPE) difference between the two slabs, which is ignored here because the ZPE contributions of the two slabs are canceled off. This cancelation occurs because the calculations of Ke et al. [35] shows that the ZPE of $NaAlH_4$ is largely due to the light hydrogen atoms; hence, the addition or substitution by Ti in the slab would have a negligible effect on ZPE value of the slab. Furthermore μ_α, the absolute chemical potential can be written as

$$\mu_\alpha = \Delta\mu_\alpha + \mu^0_\alpha = E^0_\alpha + E^{\mathrm{ZPE}}_\alpha + \Delta\mu_\alpha \qquad (3)$$

where $\mu_\alpha{}^0$ is the chemical potential of α in its most stable standard state structure. (This is the BCC-structure for Na, FCC-structure for Al, HCP-structure for Ti, and the gaseous dimer molecule for H_2). $\Delta\mu_\alpha$ is the chemical potential of α relative to that of corresponding elemental solid in the most stable structure which can be described by E^0_α, the total energy of α in its most stable structure at 0 K; and E^{ZPE}_α, which is the corresponding ZPE. Due to the negligible

(34) Frankcombe, T. J.; Lovvik, O. M. *J. Phys. Chem. B* **2006**, *110*, 622–630.
(35) Ke, X.; Tanaka, I. *Phys. Rev. B* **2005**, *71*, 024117–16.
(36) Vajeeston, P.; Ravindran, P.; Vidya, R.; Fjellvag, H.; Kjekshus, A. *Appl. Phys. Lett.* **2003**, *82*, 2257–2259.
(37) Boettger, J. C. *Phys. Rev. B* **1994**, *49*, 16798–16800.
(38) Van de Walle, C. G.; Neugebauer, J. *Phys. Rev. Lett.* **2002**, *88*, 066103.

contribution of ZPE to the total energy of elemental Na, Al, and Ti, we only calculated the $E_{H_2}^{ZPE}$ of H_2. The calculated bond length of H_2 is 0.749 Å compared with the experimental value 0.741 Å. [39] The predicted vibration frequency and ZPE are 4301.55 cm^{-1} and 0.267 eV respectively, which is consistent with the experimental values of 4401 cm^{-1} and 0.273 eV. [39] Here, $\Delta\mu_{Ti}$ is assumed to be zero, which is justified by the experimental observation that the Ti-dopant is reduced to the zerovalent state or is only very slightly oxidized. [3−7]

To correlate the surface defect formation enthalpy of (001) $NaAlH_4$ with the dehydrogenation and hydrogenation conditions (phase decomposition of $NaAlH_4$ into Na_3AlH_6 and vice versa), we utilize the method as proposed by Zhang et al.,[40] and the method is as follows.

$\Delta H_f^{NaAlH_4}$, the formation enthalpy of $NaAlH_4$, is by definition given by the energy difference between the compound and its constituent elements in their standard state. Therefore in equilibrium we have

$$\Delta\mu_{Na} + \Delta\mu_{Al} + 4\Delta\mu_H = \Delta H_f^{NaAlH_4} \quad (4)$$

The formation enthalpy can be calculated by

$$\Delta H_f^{NaAlH_4} = E_{NaAlH_4}^0 - E_{Na}^0 - E_{Al}^0 - 4(E_H^0 + E_H^{ZPE}) + E_{NaAlH_4}^{ZPE} \quad (5)$$

where $E_{NaAlH_4}^{ZPE}$ is the value of 0.8 eV per formula unit cell as calculated by Ke et al. [35]

Similarly, for Na_3AlH_6, we have

$$3\Delta\mu_{Na} + \Delta\mu_{Al} + 6\Delta\mu_H = \Delta H_f^{Na_3AlH_6} \quad (6)$$

where $\Delta H_f^{Na_3AlH_6}$ is the formation enthalpy of Na_3AlH_6. The ZPE value of Na_3AlH_6 is 1.167 eV per formula unit cell as calculated by Ke et al.[35]

To avoid the precipitation of $NaAlH_4$ and Na_3AlH_6 into its pure elemental components, we have the following additional chemical potential limits:

$$\Delta\mu_{Na} \le 0, \quad \Delta\mu_{Al} \le 0, \quad \Delta\mu_H \le 0 \quad (7)$$

We plot the above chemical potential limitations (eqs 4 and 7) in a triangular chemical phase diagram in Figure 2 by using $\Delta\mu_H$ and $\Delta\mu_{Na}$ as the *x*- and *y*-axis variables, respectively. The inside of the triangle denotes all values of $\Delta\mu_H$, $\Delta\mu_{Na}$, and $\Delta\mu_{Al}$ for which the $NaAlH_4$ compound is stable.

Furthermore, when $NaAlH_4$ is in phase equilibrium with Na_3AlH_6, we have

$$\Delta\mu_{Na}^{NaAlH_4} = \Delta\mu_{Na}^{Na_3AlH_6}, \quad \Delta\mu_{Al}^{NaAlH_4} = \Delta\mu_{Al}^{Na_3AlH_6}, \quad \ldots \quad (8)$$

To achieve this, we combine eq 4 and 6 and have

$$\Delta H_f^{NaAlH_4} + 2\Delta\mu_{Na} + 2\Delta\mu_H = \Delta H_f^{Na_3AlH_6} \quad (9)$$

The above equation can be plotted together with the phase diagram for $NaAlH_4$ in Figure 2 to yield line BD, which is the division line denoting metastable equilibrium between $NaAlH_4$ and Na_3AlH_6. If we express $\Delta\mu_H$ as an independent variable whose range is limited by eqs 7 and 9, we get

$$\frac{1}{2}(\Delta H_f^{Na_3AlH_6} - \Delta H_f^{NaAlH_4}) - \Delta\mu_{Na} \le \Delta\mu_H \le 0$$

Hence, points B and D represent the chemical potential conditions for phase transformation of $NaAlH_4$ into Na_3AlH_6 under hydrogen-poor and hydrogen-rich conditions, respectively. Following the chemical potential of the constituents on line BD, we may now use eq 2 to examine the relative thermal stability of various Ti-doped $NaAlH_4$ surface defects by using $\Delta\mu_H$ as an independent variable.

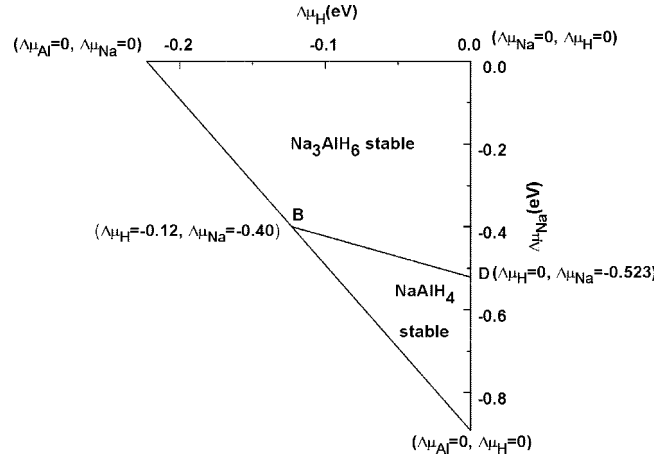

Figure 2. Calculated Ti-defect stability phase diagram of $NaAlH_4$ in metastable equilibrium with Na_3AlH_6. Points B and D denote hydrogen-poor and hydrogen-rich conditions, respectively.

Results and Discussion

Figure 3 shows the calculated surface defect formation enthalpy of Ti-doped $NaAlH_4$ (001) surface when $NaAlH_4$ is in metastable equilibrium with Na_3AlH_6. It can be seen that under both hydrogen-poor and hydrogen-rich conditions, the stable surface defect with the smallest formation enthalpy is the one in which Ti substitutes Al in the subsurface layer with an interstitial hydrogen in the vicinity ($Ti_{Al}^{sub} + H_i$). To probe the role of Ti and the interstitial H in this surface defect during dehydrogenation of $NaAlH_4$, we examine the variation in Al−H bond lengths in the Ti_{Al}^{sub} and $Ti_{Al}^{sub} + H_i$ defective slabs, respectively. Figure 4 shows the bond lengths of (a) pure $NaAlH_4$ slab, (b) $NaAlH_4$ slab with Ti at the Al site of subsurface layer (Ti_{Al}^{sub}), and (c) $NaAlH_4$ slab with Ti at the Al site of the subsurface layer and an interstitial hydrogen ($Ti_{Al}^{sub} + H_i$). It can be seen that the Al−H bond length of the two AlH_4^- units on the (001) $NaAlH_4$ slab is about 1.64 Å, as shown in Figure 4a. When Ti substitutes at the Al site (Ti_{Al}^{sub}) of the subsurface layer of $NaAlH_4$, one of the Al−H bond lengths of the two neighboring AlH_4^- units increases to 1.77 Å, while the distance between Ti and Al for defect Ti_{Al}^{sub} is 2.95 Å, as shown in Figure 4b. With the introduction of an additional interstitial H ($Ti_{Al}^{sub} + H_i$) in the slab, we note that the Al−H bond length further increases to 1.80 Å, while the Ti−Al bond lengths decrease from 2.95 Å to

(39) Huber, K. P.; Herzberg, G. G. *Molecular Spectra and Molecular Structure. IV. Constants of Diatomic Molecules*; Van Nostrand Reinhold Co., 1979.
(40) Zhang, S. B.; Wei, S.-H. *Appl. Phys. Lett.* **2002**, *80*, 1376.

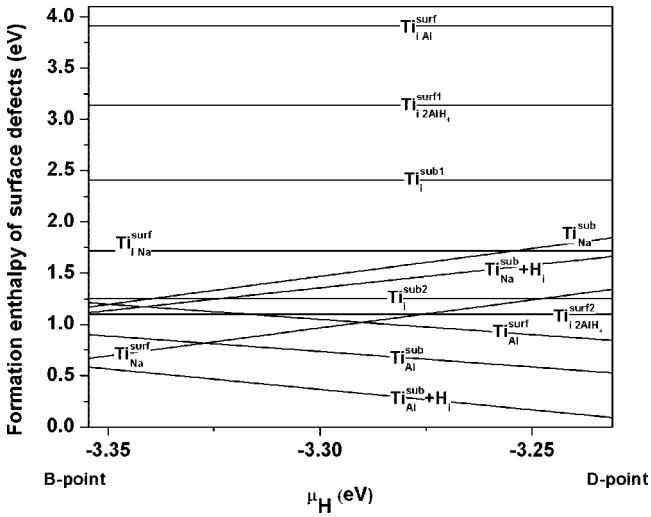

Figure 3. Calculated formation enthalpy of defects on (001) Ti-doped $NaAlH_4$ surface along BD line of Figure 2. Ti_{Al}^{surf} and Ti_{Al}^{sub} denote Ti substitution of Al in the surface or subsurface layer; Ti_{Na}^{surf} and Ti_{Na}^{sub} denote Ti substitution of Na in the surface or subsurface layer; $Ti_{i2AlH_4}^{surf}{}^{-}$, $Ti_{i2AlH_4}^{surf}{}^{-}$, Ti_{iNa}^{surf}, and Ti_{iAl}^{surf} denote Ti atoms located at surface interstitial sites; Ti_i^{sub} denotes Ti atom located in the subsurface layer interstitial site; and $Ti_{Al}^{sub} + H_i$ denotes Ti substitution of Al in the sublayer with introduction of an interstitial H atom in the vicinity of the Ti atom.

2.88−2.92 Å, which are close to the experimental range of Ti−Al interatomic distances (2.8 ± 0.02 Å) seen in EXAFS of Ti-doped $NaAlH_4$. [8] The results indicate that the interstitial H near the Ti atom may play an important role not only in enhancing the Ti−Al interactions but also in weakening the Al−H bonds simultaneously. It is also interesting that the H atom with the longest Al−H bond length (1.80 Å) is not at the surface but is at the subsurface layer beside the doped Ti. This implies that the Ti, Al and the interstitial H may work together as a Ti−H−Al cluster to facilitate AlH_3 release on (001) $NaAlH_4$, rather than releasing hydrogen on the surface. Clearly our findings are related to the widely speculated Ti−Al clusters on the surface which lower the potential energy barrier to the formation of a mobile AlH_3. [13] However, in our model, the origin of the Al−H weakening mechanism is due to the formation of Ti−H−Al clusters instead of the Ti−Al clusters. The following electronic structure calculation also proves that the interstitial H in the metastable Ti−H−Al cluster may act as a bridge to interact with Ti and Al simultaneously by local electron density transfer, which is in better agreement with the hypothesis by Kang et al. [10] However, in contrast with their conclusion, the role of Ti in our model is in the release of AlH_3 species, rather than H atoms.

We plot local or projected density of states (LDOS) of the $NaAlH_4$ slabs without and with stable surface defect ($Ti_{Al}^{sub} + H_i$) in Figure 5 a,b, respectively. The partial LDOSs of the Ti, the two Al atoms on the surface affected by Ti, and the H with the longest Al−H bond length are examined. Here we only present the up-spin DOS due to the negligible differences between the up-spin and down-spin electron densities. Our motivation for conducting a spin-polarized study is a study of Marashdeh et al. [24] that showed an energy difference for Ti-doped $NaAlH_4$ clusters in spin-polarized and non-spin-polarized calculations. The indiscernible difference between the spin-up and spin-down density of states

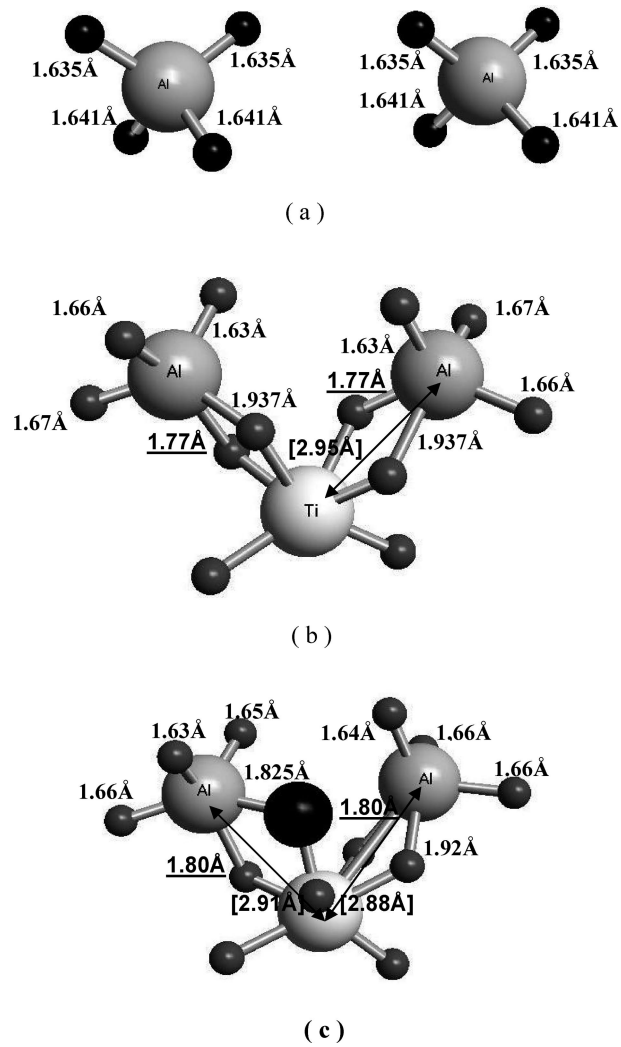

Figure 4. Bond lengths of (a) pure $NaAlH_4$ slab, (b) $NaAlH_4$ slab with Ti at the Al site of subsurface layer (Ti_{Al}^{sub}), and (c) $NaAlH_4$ slab with $Ti_{Al}^{sub} + H_i$. The small black balls and big black ball denote the H atoms in AlH_4^- and the interstitial hydrogen, respectively.

in our case probably points to the fact that spin-polarization may play a more important role in the electronic structure of clusters. For the undoped $NaAlH_4$ slab, the calculated valence band near the Fermi level is mainly composed of the s and p electrons of Al and the s electrons of H, whereas the s and p electrons of Na hybridize mainly at the antibonding conduction band. This result suggests covalent Al−H bonds within the AlH_4^- unit but a weak ionic bond between Na and AlH_4^-, which is in agreement with the electronic structure of bulk $NaAlH_4$. [19] With $Ti_{Al}^{sub} + H_i$ on the surface, it is noted that the hybridization between s and p electrons of Al and the s electron of H has decreased. The decrease in the Al−H orbital hybridization can be explained by the extra orbital overlaps between the s and p orbitals of Al with the 3d orbitals of Ti as well as between the s orbital from the interstitial H and 3d orbital from Ti. Combined with the bond length changes as discussed before, the Al−H bond weakening in $NaAlH_4$ can be described as follows: (a) the interstitial H_i in the stable defect $Ti_{Al}^{sub} + H_i$ acts as a "hand" to pull the Ti dopant closer to the surface Al atoms, which leads to the enhanced Ti−Al interaction. (b) The Ti−Al bond

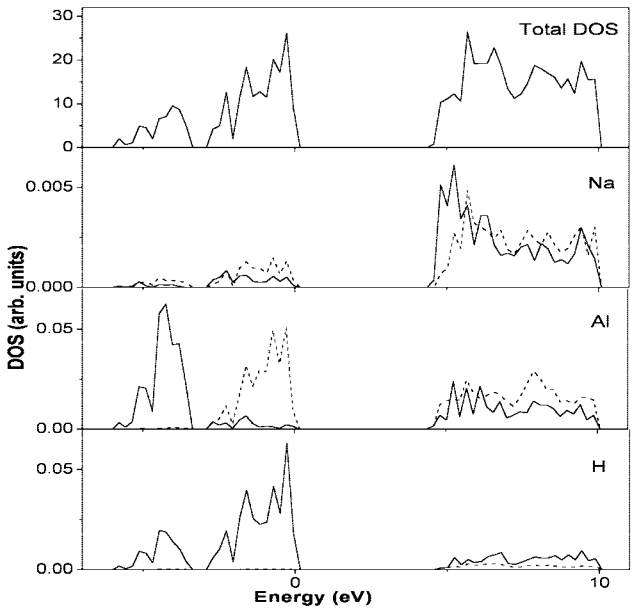

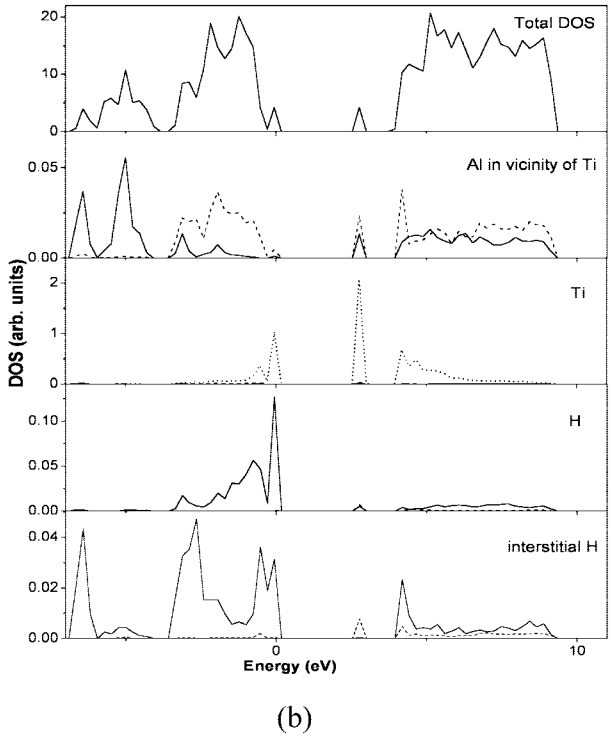

Figure 5. Density of states of $NaAlH_4$ (001) surface slab without (a) and with (b) Ti-doping ($Ti_{Al}^{sub} + H_i$). The solid line, dashed-line, and dotted line denote the s, p, and d states of each atom, respectively.

formation reduces the electron number of Al in hybridization with H, resulting in Al−H bond weakening. (c) The weakening of Al−H bond subsequently lowers the barrier of AlH_3 release, facilitating the phase transformation of $NaAlH_4$ into Na_3AlH_6.

We will now discuss the thermal stability and concentration of the stable surface defect $Ti_{Al}^{sub} + H_i$ during the hydrogenation and dehydrogenation cycles. The concentration of a defect, C, is related to its formation enthalpy, ΔH_f, by the equation $C \propto \exp(-\Delta H_f/(kT))$, where k is the Boltzmann's constant and T is the temperature in kelvin.[41] Hence, defects with high formation energy are lower in concentration and vice versa. We compare the formation enthalpy of the surface defect under hydrogen-rich and hydrogen-poor conditions and find that the surface defect thermal stability or concentration is mediated by the changing hydrogen chemical potentials during hydrogenation and dehydrogenation cycles. It is found that under the hydrogen-rich conditions (point D of Figure 2), the formation enthalpy of the stable surface defect $Ti_{Al}^{sub} + H_i$ is very small (0.08 eV). This implies that concentrations of the Ti−H−Al clusters in the $NaAlH_4$ lattice should be high and acts as a dominant active site for Al−H bond weakening. Conversely, under hydrogen-poor conditions (point B of Figure 2), the much higher formation enthalpy value (0.52 eV) implies that the concentration of $Ti_{Al}^{sub} + H_i$ is decreased, and so are the active sites involved in Al−H bond weakening. This may explain why the Ti species does not prevent hydrogenation reactions under hydrogen-poor conditions and exhibits reversible behavior under dehydrogenation and hydrogenation reactions. It is also consistent with the experimental finding that the Ti chemical environment remains invariant during the dehydrogenation/hydrogenation cycles. [8]

In light of our findings, we now understand why the use of crystalline $TiAl_3$ or TiH_2 as Ti-precursors [5,11] in the dehydrogenation of $NaAlH_4$ leads to kinetics that are not as favorable as other Ti-precursors. This is because these species are thermodynamically stable under aluminum-rich or hydrogen-rich conditions ($3\Delta\mu_{Al} + \Delta\mu_{Ti} \geq \Delta H_f^{TiAl_3}$ and $2\Delta\mu_H + \Delta\mu_{Ti} \geq \Delta H_f^{TiH_2}$, where $\Delta H_f^{TiAl_3}$ and $\Delta H_f^{TiH_2}$ are formation enthalpies of $TiAl_3$ and TiH_2, respectively) and thus do not facilitate reformation of the catalytically active cluster during formation of $NaAlH_4$ from Na_3AlH_6. The initial choice of the catalyst is thus important. Furthermore, the dehydrogenation kinetics of $NaAlH_4$ can be improved by carefully controlling the environment in which the Ti-doped $NaAlH_4$ is prepared. In this case, a slight hydrogen overpressure during mixing of Ti and $NaAlH_4$ is favorable for the generation of the stable Ti defect while avoiding the formation of TiH_2.

Conclusion

In conclusion, using first principles calculations in combination with chemical potential considerations, we have identified that the most stable defect on Ti-doped (001) $NaAlH_4$ surface is $Ti_{Al}^{sub} + H_i$, a Ti−H−Al cluster. The H in this cluster enhances the Ti−Al bonds and weakens the Al−H bonds simultaneously by bringing the Ti and Al atoms closer together. The different thermal stability of the defect under hydrogen-poor and hydrogen-rich conditions could be the origin of the exhibited reversible cyclic catalytic behavior of Ti in $NaAlH_4$. Our result presents a more realistic picture for the reversible catalytic mechanism of Ti in $NaAlH_4$, which may form the basis for the further development of catalysts for alkali metal hydrides.

CM8016038

(41) Na-Phattalung, S.; Smith, M. F.; Kim, K.; Du, M.-H.; Wei, S.-H.; Zhang, S. B.; Limpijumnong, S. *Phys. Rev. B* **2006**, *73*, 125205.